Chapter 2

Space and Ground-based Observations and Their Analysis Techniques

In this chapter, we describe briefly about various space and ground-based observatories (e.g., Solar Dynamics Observatory *SDO**; Solar TErrestrial RElations Observatory*** *STEREO**; the Big Bear Solar Observatory*** *BBSO**, etc). We also outline some details about onboard instruments on them by emphasizing their observational capabilities (e.g., Atmospheric Imaging Assembly*** *AIA**; Sun-Earth Connection Coronal and Heliospheric Investigation*** *SECCHI* ***Coronagraphs and EUV Imagers; Heliospheric Imagers, and*** *in situ* ***space weather observations). We utilize and analyze the observational data of these instruments in the present thesis. Making the selection of a variety of the appropriate observations from these space and ground-based instruments, we have accessed and analyzed them to pursue some new scientific studies presented in this thesis that demonstrate the prominence dynamics and associated physical phenomena. We also describe the data analysis techniques employed in various works presented in this thesis, e.g., the image calibration and enhancement method, some analysis***

techniques associated with Extreme Ultraviolet (EUV) imaging and Coronagraphic observations, Differential Emission Measure (DEM) analysis to determine the density and temperature structures in the solar corona, etc. We conclude about the significance of the analyzed observations and their analysis techniques in the last section.

2.1 Introduction

The Sun emits all wavelengths of the electromagnetic radiations (e.g., γ rays to the radio waves) from different layers of its atmosphere. The exterior atmosphere of the Sun has a multi-temperature view ranging from 4300 to $1-2\times10^6$ K. The multi-wavelength imaging observation is one of the strongest tools that can be utilized to explore the exterior atmosphere of the Sun. As we already know, the innermost layer of the Sun is known as the photosphere that mostly emits in the visible range (3800 – 7500 Å) of the electromagnetic spectrum. Therefore, the visible wavelength is used to observe the solar photosphere from the ground-based observatories with some atmospheric distortion. Above the photosphere, the chromosphere lies that is observable from the ground-based observatories in Hα 6563 Å and Ca II (H & K; 3934 Å, 3969 Å) lines, as well as also from the space in certain EUV emissions. The outermost layer of the solar atmosphere is known as corona with a temperature of more than a million-degree Kelvin. It is mainly observed in the Extreme Ultraviolet (EUV) and X-ray emissions. The Earth's atmosphere blocks these wavelengths, therefore, to observe the solar corona in EUV and X-ray wavebands, the space-borne telescopes are required along with appropriate detectors or spectrograph.

The solar observations have a long history and it began in the 17th century when Galileo (1610) has used his telescope to detect the sunspots on the solar surface. However, the space-based satellite observations have been started in 1946 to observe the Sun in the ultraviolet, extreme ultraviolet, and X-ray wavelengths that are not accessible from the Earth. The Orbiting Solar Observatory (OSO; 1946) series combined with Skylab (1973) had provided many important observations in the UV, EUV, and X-ray that put forward the foundation of solar space science. Later, Solar Maximum Mission (SMM) was launched in 1980 that performed the imaging and spectroscopic observations of the Sun in UV, EUV, and X-ray wavelengths to study the emissions from the hot plasma associated with the solar flares and hot corona (Bohlin et al., 1980). The Yohkoh was a Japanese mission launched in 1991 to explore the corona using soft X-ray telescope (SXT) and hard X-ray telescope (HXT). The major finding of this satellite was the detection of Masuda flare (Masuda et al., 1994), double hard X-ray source, thermal source of soft and hard X-rays, etc. Currently, many space-borne satellites are floating in the space that continuously observe the Sun in UV, EUV, and X-rays wavelengths. The Geosynchronous Operational Environmental Satellite (GOES) is a series of satellites that estimate the X-ray flux from the Sun and classify the flares (Wagner et al., 1987). The Solar and Heliospheric Observatory (SOHO) was launched in 1995 to study the internal composition of the Sun, solar atmosphere, the origin of the solar wind, and the complex interaction between the Sun and the Earth's atmosphere (Domingo et al., 1995). In the next, the Transition Region and Coronal Explorer (TRACE) was a Sun-synchronous satellite launched in 1998 to explore the connection between fine-scale magnetic fields and associated plasma structures covering from the photosphere to the solar corona (Handy et al., 1999). The Reuven Ramaty High Energy Solar Spectral Imager (RHESSI) has captured the solar flare images in wavelength of soft X-ray to hard X-rays and γ rays (Lin et al., 2002). The Hinode was launched in 2006 into a Sun-synchronous orbit to understand the mechanism behind the source region of the solar eruptions that power the solar atmosphere (Kosugi et al., 2007). The Solar TErrestrial RElations Observatory (STEREO) is a part of NASA's Solar Terrestrial Probes program (STP) to understand the origin of CMEs, their 3D evolution in the interplanetary space, and their coupling with the Earth's atmosphere (Howard et al., 2008). The Solar Dynamics Observatory (SDO) is the first mission of NASA's Living With a Star (LWS) Program to explore the solar variability and its impact on the Earth. The SOHO, HINODE, STEREO, and SDO are used to explore the Sun's atmosphere, different types of solar eruptions (e.g., prominences, jets, solar flares, etc.), MHD waves, etc. by using multiwavelength images of EUV wavebands. In the present thesis, we have used EUV emission images from Solar TErrestrial RElations Observatory (STEREO) and Solar Dynamics Observatory (SDO) to understand the prominence dynamics and their responses in the solar atmosphere. EUV observations from the space are extremely useful to understand the dynamical phenomena in the solar atmosphere at diverse spatio-temporal scales. Recently launched Solar Orbiter spacecraft will provide high-resolution EUV imaging data (spatial resolution $\approx$ 350 km). The Extreme Ultraviolet Imager (EUI) onboard Solar Orbiter releases its first images of the solar corona that explores the "campfire" (Figure 2.1) that was not observable before by other spacecrafts or ground-based observatories. The ”campfires” are the small-scale solar flares that are millions or billion times smaller than the normal flares. Therefore, the present and the future EUV imaging-related spacecrafts will have marvelous capabilities to explore the dynamical nature of a variety of magnetic structures (e.g., prominences, coronal loops, etc) in terms of their internal as well as bulk dynamics in the solar atmosphere. The Extreme Ultraviolet Imager (EUI) onboard Solar Orbiter may open a new window for understanding an individual as well as bulk dynamics of the prominence threads that have not been observed before by any other space-borne satellite. In the present thesis, we have used multi-wavelength EUV observations from space and Hα observations from the ground respectively to understand various dynamical plasma processes in the solar prominences.

The dynamical behavior of eruptive prominences and their response in the outer corona in form of coronal mass ejections (CMEs) have been explored using the visible emission coronagraphic data. The photosphere has a total brightness of 10^6 times higher than the solar corona. Therefore, to observe the solar corona in the visible wavelength, the

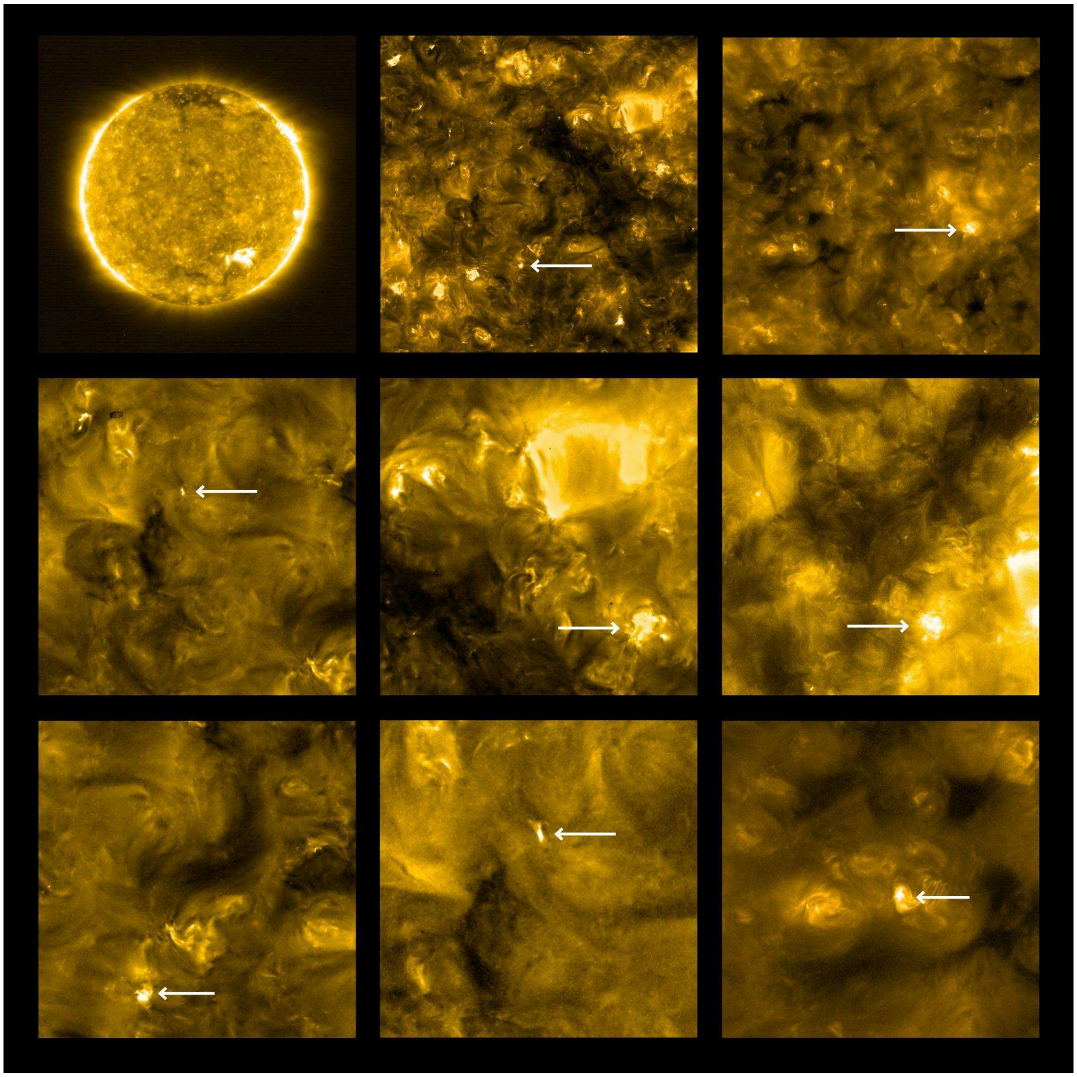

Figure 2.1: The Extreme Ultraviolet Imager (EUI) onboard Solar Orbiter will open a new window to understand many of the spectacular features that have not been observed before by other space satellites. The first image obtained from the Solar orbiter that shows the omnipresence nature of campfires on the Sun, signify the importance of EUV observations. (Courtesy: Solar Orbiter/EUI Team in ESA & NASA; CSL, IAS, MPS, PMOD/WRC, ROB, UCL/MSSL)

photosphere must be blocked by the artificial eclipse known as ”coronagraph”. The solar corona mostly emits EUV and X-ray emissions, whereas the photosphere mainly emits visible wavelengths. Large-scale solar eruptions (e.g., prominence, CMEs) consist of cool plasma that move through the outer diffused corona and can be seen using the coronagraphic observations. The photospheric light is scattered by the free electrons in the diffused outer corona. This process is known as Thompson scattering and the observation of the solar corona is performed in terms of this scattering process by measuring the total brightness. The first coronagraph was used by Bernard Lyot in 1931 to observe the solar corona. After the launch of the human-based program of Skylab to observe the Sun, some more space-borne telescopes were, Solwind coronagraph onboard P78-1 (1978–1985) and the Solar Maximum Mission (1984–1989). Currently, four space-borne coronagraphs at different locations in the heliosphere are in operation. The Large Angle and Spectrometric Coronagraph (LASCO) onboard SOHO have two coronagraphs LASCO/C2 with the field of view $2-6$ $R_\odot$ and LASCO/C3 having a field of view of $3-32$ $R_\odot$. The four other coronagraphs are lying on the Sun-Earth Connection Coronal and Heliospheric Investigation (SECCHI) onboard STEREO-A & B. The two coronagraphs are COR1 having a field of view of $1.3-4$ $R_\odot$ and COR2 with a field of view of $2.5-15$ $R_\odot$. In the series of upcoming coronagraphic observations, Solar orbiter mission is having METIS coronagraph, while PROBA-3 will have ASPIICS coronagraph ($1.08-3.0$ $R_\odot$). The upcoming Aditya-L1 Indian space mission will have onboard Visible Emission Light Coronagraph (VELC) with a field-of-view of $1.03-3.0$ $R_\odot$. The EUV imager and coronagraphic observations jointly can explore the origin, propagation, and outer atmospheric response of solar eruptive phenomena. This thesis invokes multi-wavelength imaging observations and coronagraphic observations to understand and present a variety of scientific results related to the prominence dynamics.

In this chapter, we are introducing briefly the instruments and data analysis techniques that are used to study the solar eruptive prominences. Currently, there are many sources to get high-resolution and high cadence data from different space-borne and ground-based observatories. These data are useful to study the dynamical properties of plasma, MHD plasma processes (e.g., reconnection, instabilities, eruptions, etc.), and their influence in the solar atmosphere. We have used EUV images and white-light coronagraphic images in the scientific results described in various chapters of this thesis, which are obtained from the space-borne satellites. The Atmospheric Imaging Assembly (AIA) onboard Solar Dynamics Observatory (SDO) is the main source of the data, which is used to understand the dynamics and associated plasma processes to the eruptive prominence/filaments in the lower solar corona (cf., Chapters 3-5, and Chapter 7). The influence of these large-scale eruptive prominences and associated Coronal Mass Ejections (CMEs) is also observed by the Solar TErrestrial RElations Observatory (STEREO) from lower corona to the interplanetary space (cf., Chapter 6 and 7) using its variety of instruments, e.g., Extreme Ultraviolet Imager (EUVI), Coronagraphs (COR-1 & 2), and Heliospheric Imagers (HI-1 & 2). Some images are also taken and analyzed from the Global Oscillation Network Group (GONG) Hα ground-based observations to make a qualitative understanding of the filament in the chromospheric region (cf., Chapter 7). Some data related to the space weather and geoeffectiveness have been taken from NOAA Space Weather Prediction Center, World Data Center for Geomagnetism, Kyoto University, and WIND (cf., Chapter 7). Some descriptions about the utilized instruments, their data, and some observational analysis techniques are described in detail in the next sections.

2.2 Solar Dynamics Observatory (SDO)

The Solar Dynamics Observatory (SDO; Pesnell et al., 2012) is a NASA space-borne geosynchronous orbital mission, which provides full-disk images of the Sun in the multi-temperature filters. It was launched on February 11, 2010, operated by the Goddard Space Flight Center (GSFC, NASA). This observatory is the first part of the Living With a Star (LWS) program of NASA. The main goal of the LWS program is to understand the Sun-Earth relation and its impact on human society. The main goal of the SDO is to understand the initiation and release of magnetic energy in the form of small to large-scale eruptions, MHD waves, instabilities, generation and structuring of Sun's magnetic field, etc., in the solar atmosphere and explore how these solar activities affect the Earth. The Solar Dynamics Observatory contains three instruments, the Atmospheric Imaging Assembly (AIA), the Heliospheric and Magnetic Imager, and the Extreme Ultraviolet Variability Experiment (EVE) (Figure 2.2) and develop in the collaboration with the Lockheed Martin Solar and Astrophysics Laboratory, the Stanford University, and the University of Colorado at Boulder's Laboratory for Atmospheric and Space Physics (LASP) respectively. All three instruments of SDO provide high-resolution spatio-temporal full-disk imaging data, which can be used to understand the fine structure dynamics of the solar atmosphere and their magnetic connectivity. In this thesis, we have used multi-wavelength imaging observational data from the Atmospheric Imaging Assembly (AIA; Lemen et al., 2012) to study the dynamical behavior of eruptive prominences.

2.2.1 Atmospheric Imaging Assembly

The Atmospheric Imaging Assembly (AIA; Lemen et al., 2012) onboard the Solar Dynamics Observatory (SDO) provides full-disk images of Sun in the seven Extreme Ultraviolet wavelengths (94 Å , 131 Å , 171 Å , 193 Å , 211 Å , 304 Å, and 335 Å) with an spatial resolution of 1.5" and 12 seconds temporal cadence. It also provides full-disk images in two ultraviolet (1600 Å , 1700 Å) and one in visible region (4500 Å) that observe the lower solar atmosphere (Figure 2.3). It observes the multi-temperature structure ranging from 5000 K to 20 MK of the solar atmospheres. In the present thesis, we have used different EUV filters of SDO/AIA to observe the dynamical behavior of the eruptive prominences and their impact on the solar atmosphere. The AIA 94 Å wavelength is emitted by Fe (XVIII) that peaks at a temperature of more than 6 MK, and represents the solar corona during a solar flare (Figure 2.3). The AIA 131 Å filter has two peaks at a temperature of 0.5 and 10 MK, emitted by Fe(VIII/XXI), and observes the transition region as well as the

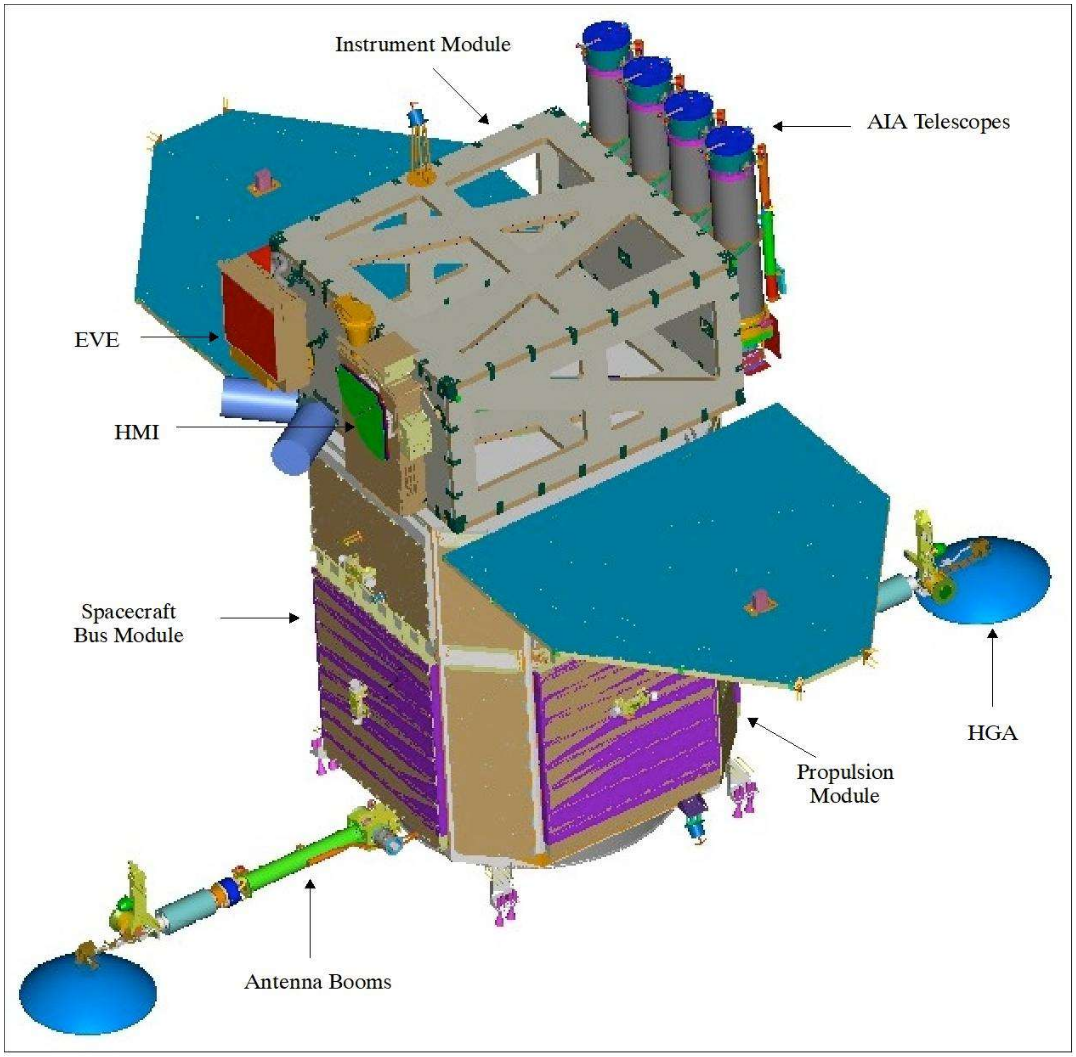

Figure 2.2: An image of SDO spacecraft. The SDO spacecraft consists of three instruments, the Atmospheric Imaging Assembly (AIA), the Heliospheric and Magnetic Imager, and the Extreme Ultraviolet Variability Experiment (EVE) that simultaneously probe the different layers of the solar atmosphere. (Courtesy: NASA)

flaring region of the solar corona (Figure 2.3). Similarly other EUV filters like 171 Å, AIA 193 Å, AIA 211 Å, AIA 304 Å, AIA 335 Å peak at temperature of 0.6 MK, 1 & 20 MK, 2 MK, 0.5 MK, 2.5 MK, emitted from the ions Fe (IX), Fe (XII & XXIV), Fe (XIV), He (II), Fe (XVI), and represent the quiet region/upper transition region, the corona/hot flare plasma, the active region corona, the upper chromosphere, and the active region corona respectively. The ultraviolet wavebands (AIA 1600 Å, AIA 1700 Å) are emitted by C (IV), ultraviolet light continuum at a temperature of 10000 K, 5000 K, and observe the transition region and upper photosphere where the temperature minimum is appeared (Figure 2.3). The AIA 4500 Å is emitted from the white light continuum, shows a visible surface of the Sun or photosphere.

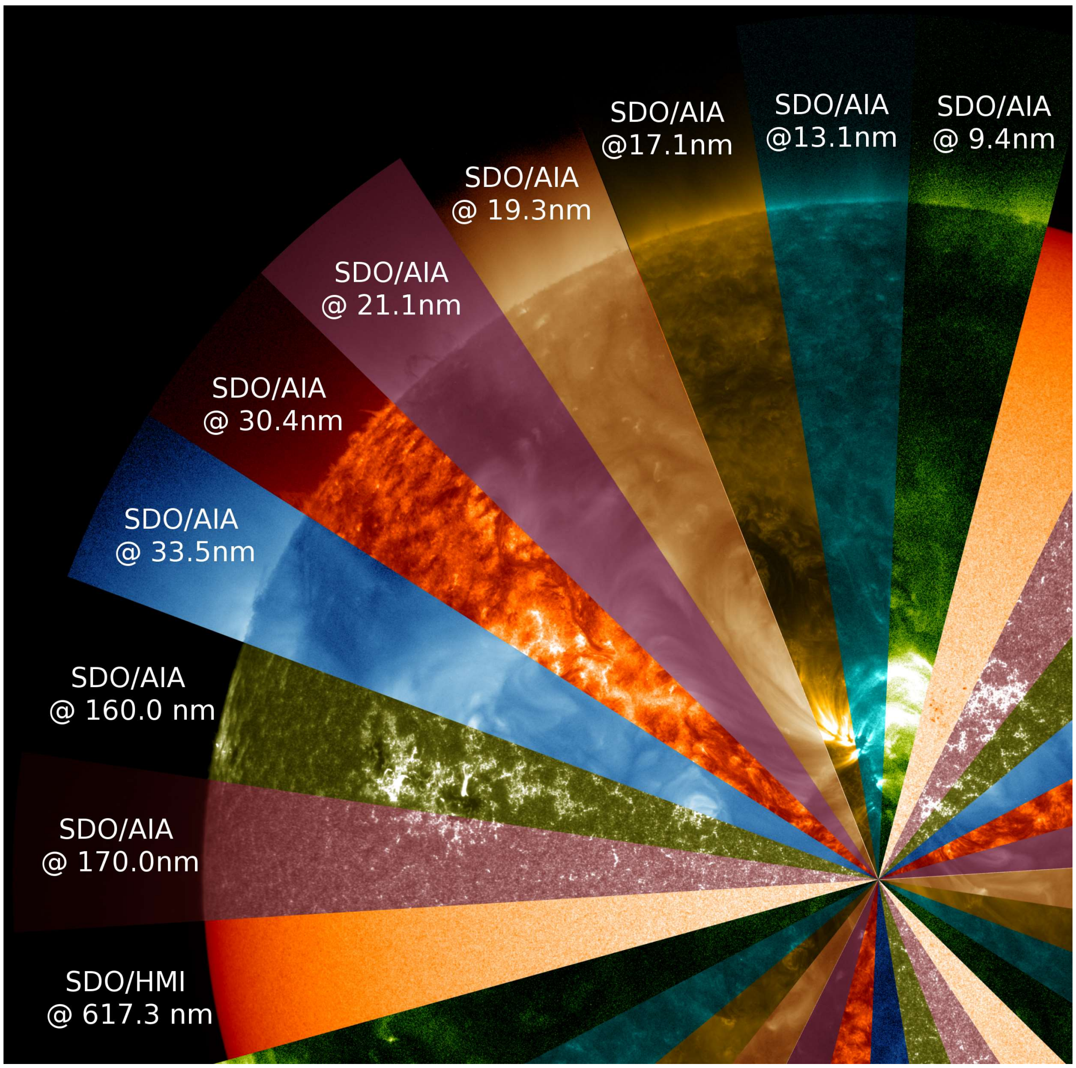

Figure 2.3: Multiwavelength images of AIA instrument, which observe the different region of the Sun. (Courtesy: https://solarsystem.nasa.gov/)

The AIA telescope observes the Sun up to 0.5 $R_\odot$ above the solar limb with a pixel length of 0.6" pixel^{-1}, having a spatial resolution of 1.5", and a cadence of 12 seconds for EUV wavebands. It consists of four Cassegrain telescope, which is optimized to observe the narrow band EUV filters to observe the solar atmosphere. Each telescope has a 20 cm primary mirror and an active secondary mirror. Each telescope contains a front door, a focus mechanism, a filter wheel, a shutter mechanism, and a 4096×4096 pixel CCD camera, which captures the Sun images at the regular interval. The front door protects the filters from debris and acoustic load during the launch. During the focus mechanism, the secondary mirror adjusts the primary mirror along the optical axis and the filter wheel provides a tool to select the desired filters. The shutter mechanism consists of a 159 mm diameter thin blade that rotates to open the shutter, exposing the CCD. The CCD captures an image of a 4096×4096 pixel image of Sun with 12 seconds cadence. These high-resolution images of the Sun in ten wavebands are useful to reveal the key aspects of solar activity. The high-speed camera on AIA can capture the small to larger-scales rapid magnetic activities (e.g., jets, prominences, solar flares, CME, etc) and their initiation. It can also be useful to understand that how the solar storm is initiated near the Sun and causes the coronal heating. Most of the solar storm is related to the large-scale eruptions (e.g., prominence, CME, solar flares). The AIA data with a combination of Solar Terrestrial Relations Observatory (STEREO) can be used to understand the 3D evolution of prominence and coronal mass ejections in the solar corona.

We use aia_prep routine available in Solarsoft for the basic calibration and normalization of the AIA data. The aia_prep normalized the level 1 data to level 1.5. It updated the header and perform the basic calibration like rotation, translation, scaling of the data. We downloaded the SDO/AIA data from the Joint Science Operation Center (http://jsoc.stanford.edu/), which acts as a data-distribution center handled by the Stanford University.

In the next section, we describe about the Solar TErrestrial RElations Observatory (STEREO) and its onboard instrument suites.

2.3 Solar TErrestrial RElations Observatory (STEREO)

Solar TErrestrial Relations Observatory (STEREO) is the third space mission of the NASA's Solar Terrestrial Probes program that provides the stereoscopic images of the Sun. Two identical spacecrafts (STEREO-A and STEREO-B) was launched by the NASA on the 26^{th}, October 2006 in the heliocentric elliptical orbit at ≈1 AU from the Sun (Figure 2.4). One is moving ahead of the Earth (STEREO-A) and one is drifting behind. As a result, each satellite moves around the Sun relative to the Earth in the opposite direction and provides a 360° view of the Sun. The spacecraft moving ahead in the Earth orbit is referred as STEREO-A and the second spacecraft behind is known as STEREO-B. The spacecraft STEREO-A take 347 days to complete one revolution around the Sun and the angle between spacecraft/Sun/Earth increases at 21.650 degrees/year. While the STEREO-B takes 387 days to complete one revolution and the spacecraft/Sun/Earth angle change -21.999 degrees/year. The two spacecraft (STEREO-A and STEREO-B) continue to separate with each other with ≈44 degrees/year. In addition to Solar Dynamics Observatory (SDO), the two spacecraft provide a full view of the Sun for several years (Figure 2.4).

The STEREO spacecraft provides the stereoscopic images of the Sun and even it observes that part of the Sun also, which is not visible from the Earth. The main science goal of the STEREO mission is to understand the 3-D evolution of coronal mass ejections from the lower corona to the interplanetary space and also their responses to the Earth's atmosphere. They monitor those CMEs also, which are initiated at far side of the Sun, massive solar wind burst, magnetic field, and solar plasma ejected from the Sun. To achieve these goals, the STEREO has four instrument suites onboard (Figure 2.5, left panel).

Sun-Earth Connection Coronal and Heliospheric Investigation (SECCHI): It consists of an extreme ultraviolet imager (EUVI), two coronagraphs (COR1

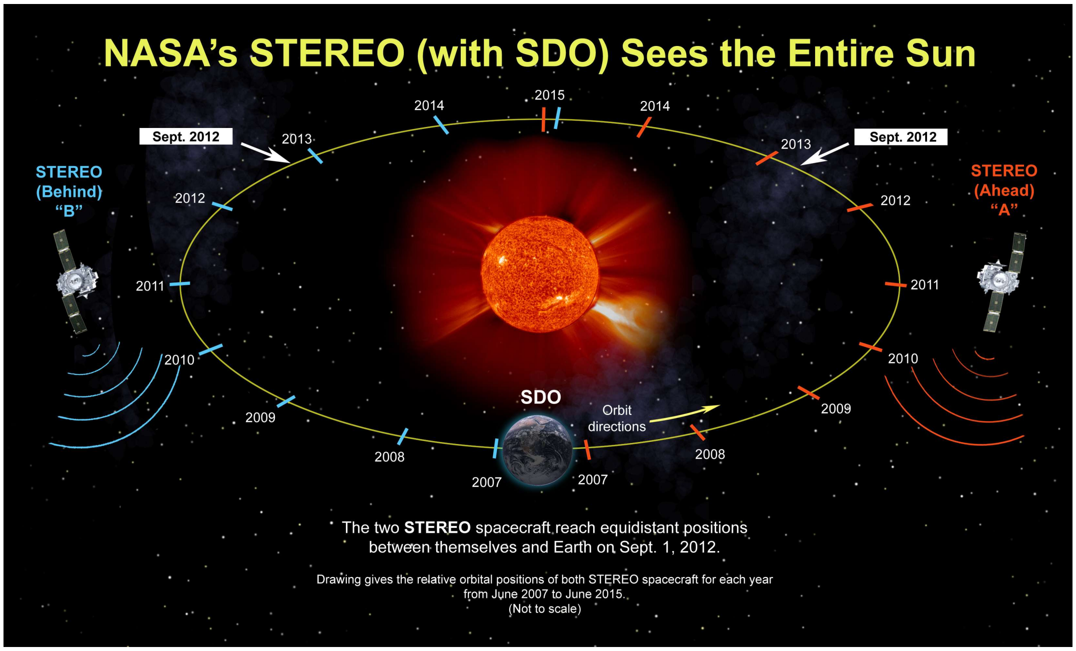

Figure 2.4: Location of spacecraft STEREO-A and STEREO-B drifting away from each other to observe the different views of the Sun. In the combination of STEREO and SDO, these two spacecraft observe the entire Sun for several years. (Courtesy: NASA/GSFC)

and COR2), and two heliospheric imagers (HI1 and HI2), which capture the stereoscopic images of the Sun from the inner corona up to the interplanetary space (215 $R_{\odot}$). The purpose of the SECCHI is to understand the initiation, development, eruption, their 3D morphological evolution and their whole journey from the Sun's surface to the interplanetary space (Figure 2.5, right panel).

In-situ Measurements of Particles and CME Transients (IMPACT): The IMPACT contains seven instruments that monitor the 3-D distribution of the solar wind plasma, the properties of solar energetic particles (SEP), and the local vector magnetic field.

PLAsma and SupraThermal Ion Composition (PLASTIC): It is used to understand the plasma characteristics of protons, alpha particles, and other heavy ions.

The PLASTIC instruments sample the solar wind and superthermal particles, and provide their kinetic behavior and composition.

STEREO/WAVES (SWAVES): The SWAVES track and probe the CME driven shock waves and flare electrons to predict how a CME interacts with the Earth and some CME properties that govern the geo-effectiveness.

In this thesis, we have used STEREO/SECCHI data to understand the dynamical nature of the eruptive prominences, their relationship with the CME, and their response in the heliosphere. In the next sub-section, we outline some details of the SECCHI and its instruments.

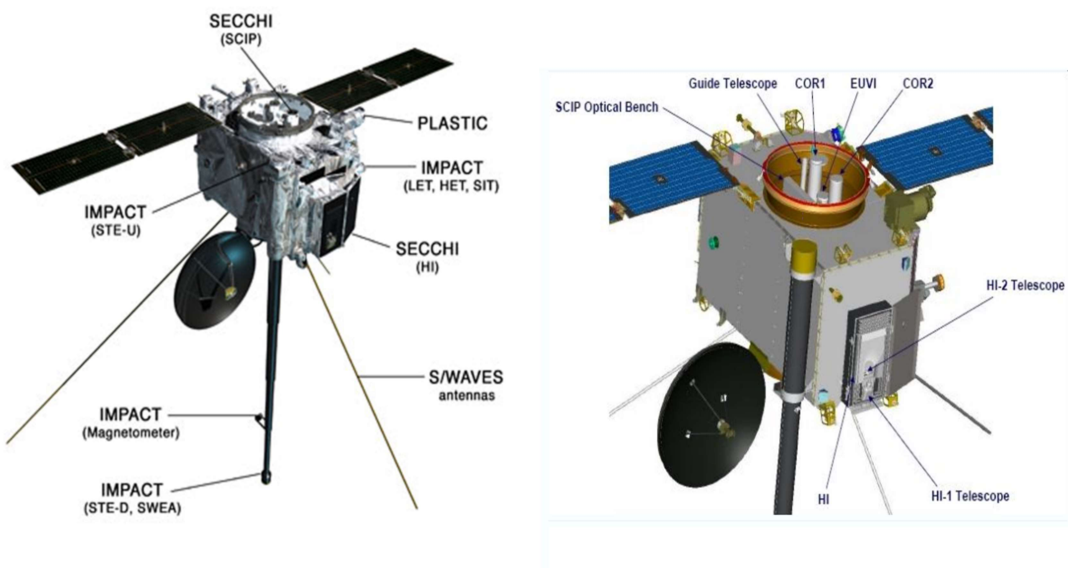

Figure 2.5: Left panel: Image of different instruments onboard the STEREO spacecraft. Right panel: Image of the SECHHI instrument onboard the STEREO and its main components. (Courtesy: NRL/NASA)

2.3.1 Instruments on Sun-Earth Connection Coronal and Heliospheric Investigation (SECCHI)

The Sun-Earth Connection Coronal and Heliospheric Investigation (SECCHI) consists of a set of five telescopes that track the solar features from the lower corona to the heliosphere (Howard et al., 2008; Wuelser et al., 2004). The EUVI telescope in combination with two coronagraphs (COR1 and COR2) is called SCIP (Figure 2.5, right panel). The SECCHI is used to observe the 3D evolution of solar structure e.g., prominences, CMEs, plumes, coronal loops, etc. The details about the five telescopes are discussed below.

The Extreme Ultraviolet Imager (EUVI): The EUVI captures the images of the Sun in four different wavelengths; 171 Å, 304 Å, 284 Å, and 195 Å. It has a normal-incidence Ritchey-Chrétien telescope with metal filters, a multi-layer coated mirror, and a 2096×2096 pixel CCD. Figure 2.6 shows the cross-sectional view of the EUVI telescope onboard SECCHI/STEREO. The light enters through the primary mirror and passes by the thin metal filters, which remove the UV, visible, and IR radiation to avoid the heating of the telescope. The multi-layer reflecting coated mirror is used to optimize the telescope for EUV lines. The rotating shutter blade controls the exposure time. Finally, the images are captured by the CCD with a spatial resolution of 1.6” and variable temporal resolution.

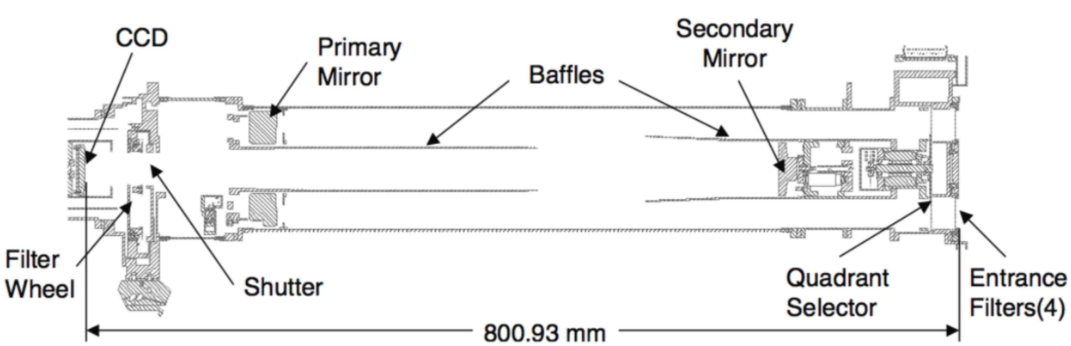

Figure 2.6: Internal view of the EUVI telescope onboard STEREO. (Courtesy: Wuelser et al. (2004)).

Coronagraphs (COR1 and COR2): The coronal brightness decreases sharply with height in the solar atmosphere. Therefore, the STEREO/COR1 telescope is used to observe the inner corona (FOV; $1.4-4\ R_\odot$), while COR2 observe the outer corona (FOV; $2-15\ R_\odot$). The COR1 is a classic Lyot internally occulting refractive coronagraph (Howard et al., 2008). The main goal of the COR1 is to explore the inner corona (FOV; $1.4-4\ R_\odot$) in white light (spectral range; 650 – 750 nm) and polarization precision. The spatial resolution of COR1 is 7.5 " and temporal resolution is 5 minutes. After every five minutes, COR1 captures the three consecutive images with a time interval of 9 seconds to observe the polarization brightness.

The COR2 coronagraph captures the images of the outer corona ($2-15\ R_\odot$). It observes the weak coronal signal in visible light by an externally occulted Lyot coronagraph, which follows after the significant observations of highly successful SOHO/LASCO C2 and C3 coronagraphs (Brueckner et al., 1995). The main goal of the COR2 coronagraph is to observe the CME in polarization brightness (pB) with a spatial resolution of 15".

Heliospheric Imagers (HI1 and HI2): The Heliospheric Imager (HI) package consists of two small, wide-angle telescopes (HI1 and HI2), which observe the heliosphere from the Sun to the Earth ($12-215\ R_\odot$) in the visible-light (Howard et al., 2008). The main objective of the HI package is to observe a CME or any other structure as they pass from the corona to the interplanetary space. The HI assembly contains the exterior baffle systems, the hinged baffle cover, the focal plane packages, the HI camera, the CCDs, which capture the heliospheric images of 2048×2048 pixel.

2.4 Global Oscillation Network Group (GONG)

The Global Oscillation Network Group (GONG) program is a combination of six ground-based observatories i.e., Teide Observatory (Canary Islands), the Learmonth Solar Observatory (Western Australia), the Big Bear Solar Observatory (California), the Mauna

Loa Solar Observatory (Hawaii), the Udaipur Solar Observatory (India), and the Cerro Tololo Inter-American Observatory (Chile). This network is used to understand the solar internal structure and dynamics. From 2010, it has been made enable to capture the image of the Sun in Hα emission, which is useful to study solar prominence and their dynamical behavior in the chromosphere. We have used GONG Hα (Harvey et al., 2011) data (cf., Chapter 7) from the Big Bear Solar Observatory (BBSO) site, which provides the full-disk images of the Sun with a spatial resolution of 2” and with 1-minute temporal cadence.

2.5 Space Weather Data

The eruptive prominence may lead geo-effective CMEs. In Chapter 7 of this thesis, we use some space weather data to describe the geo-effectiviness of CMEs. The brief details of these data sources are given below.

2.5.1 WIND

The Wind spacecraft was launched in 1994 to understand the behavior of the solar-terrestrial plasma environment, respond of the Earth’s atmosphere when it interacts with the solar wind. It measures the solar wind properties near the Earth. It has nine instruments i.e., Gamma-Ray Burst Investigation KONUS, the Magnetic Field Investigation the Solar Wind and Suprathermal Ion Composition Experiment (SMS), The Energetic Particles: Acceleration, Composition, and Transport (EPACT) investigation, the Solar Wind Experiment (SWE), a Three-Dimensional Plasma and Energetic Particle Investigation (3DP), the Transient Gamma-Ray Spectrometer (TGRS), and the Radio and Plasma Wave Investigation (WAVES). We have used Wind Magnetic Field Investigation (MFI; Bougeret et al., 1995; Farrell et al., 1995; Leinweber et al., 2008) to conjecture the average magnetic field [$\mathbf{B}$] and its components [B_x, B_y, B_z] at one-minute interval.

2.5.2 The World Data Center for Geomagnetism, Kyoto University

The World Data Center for Geomagnetism, Kyoto University, is operated by the Data Analysis Center for Geomagnetism and Space Magnetism Japan (http://wdc.kugi.kyoto-u.ac.jp/dst_realtime/index.html) that provides a catalog to measure the Dst index at an interval of one hour. Dst index is associated with the strength of the ring current around Earth caused by solar energetic particles, and provides an specific indicator about the space weather.

2.5.3 Space Weather Prediction Center (SWPC)

The planetary K index or Kp index is used to categorize the intensity of the geomagnetic storm. It measures the disturbance in the planetary magnetic field and used by Space Weather Prediction Center (SWPC; https://www.swpc.noaa.gov/products/planetary-k-index) to predict the geomagnetic storm. It is obtained from the maximum disturbance in the horizontal component of Earth's magnetic field observed on a magnetometer with a three-hour time interval. The Kp index quantifies the fluctuations in the horizontal component of Earth's magnetic field between 0 – 9 with below 4 indicate the calm weather whereas 5 or above represents an intense geomagnetic storm.

In the next section, we will describe some data analysis techniques empolyed in the different works presented in this thesis.

2.6 Data Analysis Techniques

In the present thesis, we mainly study the dynamical behavior of the eruptive prominences and their effect on the outer solar atmosphere. We also deal with some MHD plasma processes like a reconnection, instabilities that can play a crucial role in the eruptions of the prominences. To understand these phenomena and physical processes, we have used multiwavelength observations from the SDO in combination with the STEREO to understand the evolution of instabilities, reconnection in prominences, and their dynamical responses in the solar atmosphere. We observe the evolution of magnetic Rayleigh-Taylor (MRT) instability, Kelvin-Helmholtz instability, and effect of the reconnection in different types of prominences (e.g., the active region prominence, the quiescent prominence, and the polar crown prominence).

We have used high-resolution and high cadence data obtained from the Atmospheric Imaging Assembly (AIA) onboard Solar Dynamics Observatory (SDO) to derive the scientific results presented in this thesis. We use seven EUV filters (e.g., 94 Å, 131 Å, 171 Å, 193 Å, 211 Å, 304 Å, 335 Å) for multiwavelength analysis and to understand the thermal behavior of the prominences. The basic calibration of the AIA data is available on the webpage (https://www.lmsal.com/sdodocs/doc/dcur/SDOD0060.zip/zip/entry/) and discussed by (Boerner et al., 2012). The initial calibration and correction of the AIA data has been performed in three levels i.e., level 0, level 1.0, and level 1.5.

- The level 0 data is raw elementary data.
- The elementary data is processed by removing the bad pixels and flat field corrections and we obtain a level 1.0 data that is in FITS file format.
- The aia_prep routine available in the Solarsoft is applied on the level 1 data to construct the level 1.5 data. The aia_prep routine normalize the data, also update the header, and perform the basic calibration like rotation, translation, scaling of the data.

The basic calibration and normalization of STEREO data have done by the routine secchi_prep.pro that is also available in the Solarsoft library. The SECCHI images contain three levels of calibration i.e., level 0.5, level 1, level 2, respectively. The secchi_prep.pro routine performs despiking of the data, flat field, and roll angle corrections. In the next subsection, we discuss an image enhancement technique that is useful to resolve fine structures of the prominences in various imaging observations.

2.6.1 Image Enhancement

The Extreme Ultraviolet (EUV) and coronagraphic images of the corona contain several thin structures on different spatial scales and much information in different brightness regime. The multi-Gaussian image enhancement technique is used to observe the thinner and fine-scale structures that are not achievable from normal intensity images. The processed images are used to resolve the finer structures, dynamical features on different spatial scales in the eruptive prominence, filament channel, active regions, quiet-region of the Sun, and coronal mass ejection. The Gaussian kernel is used to convolve each image. The convolved images are subtracted from the normal intensity image to obtain features with better contrast. The same process has been used for multiple times to measure the

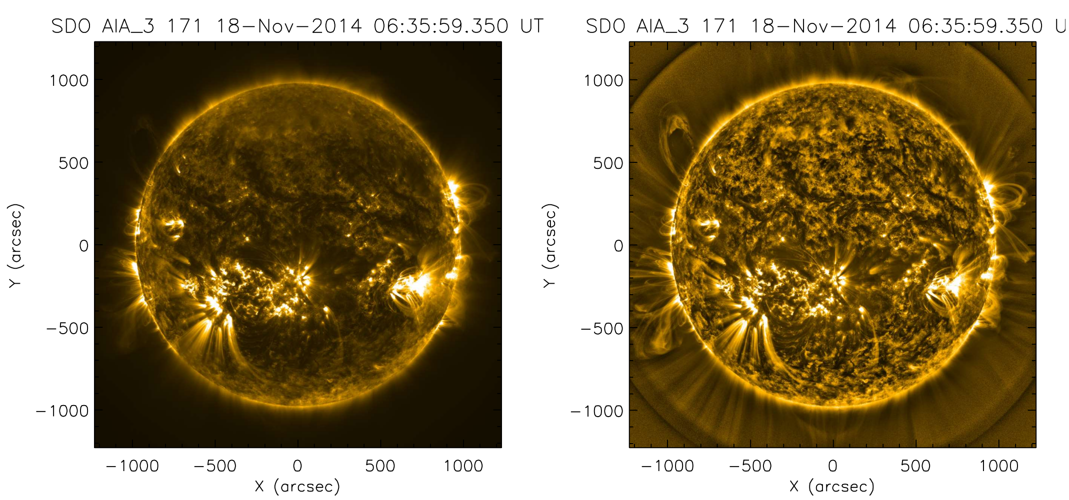

Figure 2.7: The left panel shows the normal SDO/AIA 171 Å image. The right panel shows the Multi-scale Gaussian normalization processed SDO/AIA 171 Å image. The processed image shows the more fine-scale structures in the solar corona.

uncorrelated noise. The uncorrelated noise is subtracted from the original images. We have used a normalized multiscale Gaussian filter to enhance the fine structures (Morgan and Druckmüller, 2014). We select the width of the Gaussian filter as [50, 100, 150, 200, 250] pixels. The filtered image and original image is added. Therefore, we perform the analysis using the multi-Gaussian filtered images. The normal image of AIA 171 Å filter (Figure 2.7, left panel) and enhanced image is shown (Figure 2.7, right panel). Large number of fine-scale structures, thin magnetic arcades, coronal loops can be resolved in the intensity images by employing this technique. To understand the fine-structure dynamics of the solar prominence, we have employed this technique in our works (e.g., see Chapter 3). In the next section, we present some details of Tie-pointing Method to estimate the kinematics of eruptions using STEREO observations.

2.6.2 Tie-pointing Method

To understand the dynamical evolution of prominences, coronal mass ejections and their 3D geometry in the solar corona, we have to know their exact location, height, position, etc. of a feature in the line of sight plane (LOS; SDO image) and in the projected plane (STEREO image). We select two images of the two spacecrafts (STEREO-A&B/COR1) with the same field of view at the same time. The triangulation technique is used to define a plane known as the epipolar plane by taking the images from the two different spacecrafts. The epipolar plane consists of three points, two positions from two different spacecrafts, and a third point lying at the Sun's center. These epipolar planes are seen along the line of sight (LOS). Therefore, these planes look like a line called as epipolar lines. The point at which these epipolar lines cut each other from two images of two spacecraft is known as tie-point. We use the tie-pointing method to obtain the real height, exact location, and position of the by knowing the solar coordinates. The tie-pointing method use scc_measure routine written in the Interactive Data Language (IDL) available in the Solarsoft SSW library. The scc_measure routine written in IDL by (Thompson, 2009) to locate the position of two spacecraft as two view-points of the two observers. It takes .fits or .fts file as input and displays the two images. These .fits file contain the world coordinate system (WCS) keywords, which allow the observer to obtain the real height, exact location, and position of the features in the solar corona. A 3D reconstruction technique has been used by tracking the line of sight ray that belongs to one spacecraft and back-traced into the second spacecraft of image. The intersection of two lines (tie-point) gives the exact location and real height of the features. We have selected a point on the first image (Figure 2.8; + sign on STEREO-A image) and the epipolar line that cut at tie-point shown on the other image (Figure 2.8; + sign on STEREO-B image), which passes through the same feature (Fig. 2.8). This analysis is utilized for example in Chapters 6 and 7 of this thesis.

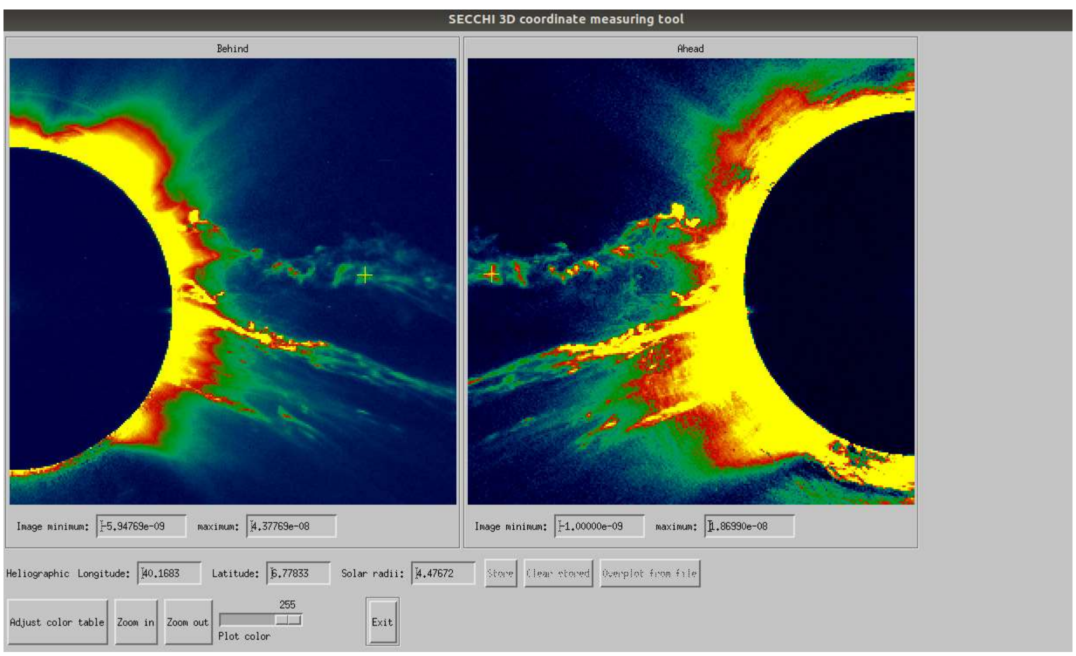

Figure 2.8: The left panel shows the STEREO-B image of an eruptive prominence. The right panel shows the STEREO-A image. The + signs in both images are lying on the same epipolar plane and provides the exact location of the feature.

2.7 Thermal Structure and Density Estimations in the Lower Corona

The solar atmosphere consists of multi-temperature magnetized plasma. These magnetized plasma are observed by the different spectral lines, which are temperature sensitive and provide crucial information about the solar atmosphere. Observations from the different space-borne telescopes (e.g., Hinode/XRT, EIS, SDO/AIA) provide a broad view of solar emission from different part of the Sun. These solar emissions widely cover a broad range of temperatures. The UV/EUV/XRT emissions from the Sun are optically thin and in the thermal equilibrium. Therefore, the thermal structure of multi-thermal plasma of the solar atmosphere can be described in terms of Differential Emission Measure (DEM). The DEM is defined as,

$$DEM(T) = \int n^2 \frac{dh}{dT} \tag{2.1}$$

where $DEM(T)$ is differential emission measure (DEM) at temperature T and at a depth of h along the line of sight, $n(h(T))$ is electron density at a depth of h and temperature T. We use two techniques of DEM analysis to understand the thermal structure of the prominences and their associated dynamics in the lower corona. The multi-wavelength observation from different space-borne telescope provides the information of multi-temperature descriptions of the prominence. The prominence plasma is associated with the cool core and hot prominence-corona transition region (PCTR). The emission from the PCTR region is mainly lying in the UV/EUV wavelength, which is emitted by the optically thin plasma. The PCTR has a small contribution in the whole mass of the prominences. However, due to the presence of the interface, PCTR needs special attention. The maximum fraction of mass of the prominences is associated with the cool core. But the cool core of the prominence (5000 – 15000 K) is not in thermal equilibrium and the emission comes from this region is optically thick. Therefore, the response function and the DEM has not correctly described the temperature distribution of plasma.

2.7.1 Regularized Inversion Method

The Hannah and Kontar (2012) method is used to understand the thermal structure by measuring the differential emission measure from the prominence and surrounding coronal magnetic field. It uses a regularized inversion method to construct the DEM of the solar observations and provides reliable horizontal and vertical error bars. The regularized DEM is obtained automatically from the regularized inversion of the SDO/AIA EUV filters as a function of temperature (T). The observed flux F_i at temperature T from different i^{th} filters of SDO/AIA is defined as,

$$F_i = \int DEM(T)R_i(T)dT + \delta F_i \tag{2.2}$$

where $DEM(T)$ is differential emission measure (DEM) at temperature T, R_i is temperature response of i^{th} filters (Figure 2.10) of SDO/AIA (Boerner et al., 2012; O'Dwyer et al., 2010) and δF_i is error in the flux. To obtain the global minimum, the χ^2 minimization is adopted, which is defined as the difference between observed and predicted count. Hannah and Kontar (2012) have used different types of regularized inversion (e.g., zeroth-order, second-order, and maximum entropy regularization). However, we use a zeroth order of regularized inversion to deduce the regularized DEM as a function of temperature. We recover the differential emission measure (DEM) map from six AIA filters including 94 Å (Fe X,~1.1 MK; Fe XVIII, ~7.1 MK), 131 Å (Fe VIII, ~0.4 MK; Fe XXI, ~11 MK), 171 Å (Fe IX, ~0.6 MK), 193 Å (Fe XII, ~1.6 MK), 211 Å (Fe XIV, ~2.0 MK) and 335 Å (Fe XVI, ~2.5 MK) using the regularized inversion method (Figure 2.9). For the inversion, the

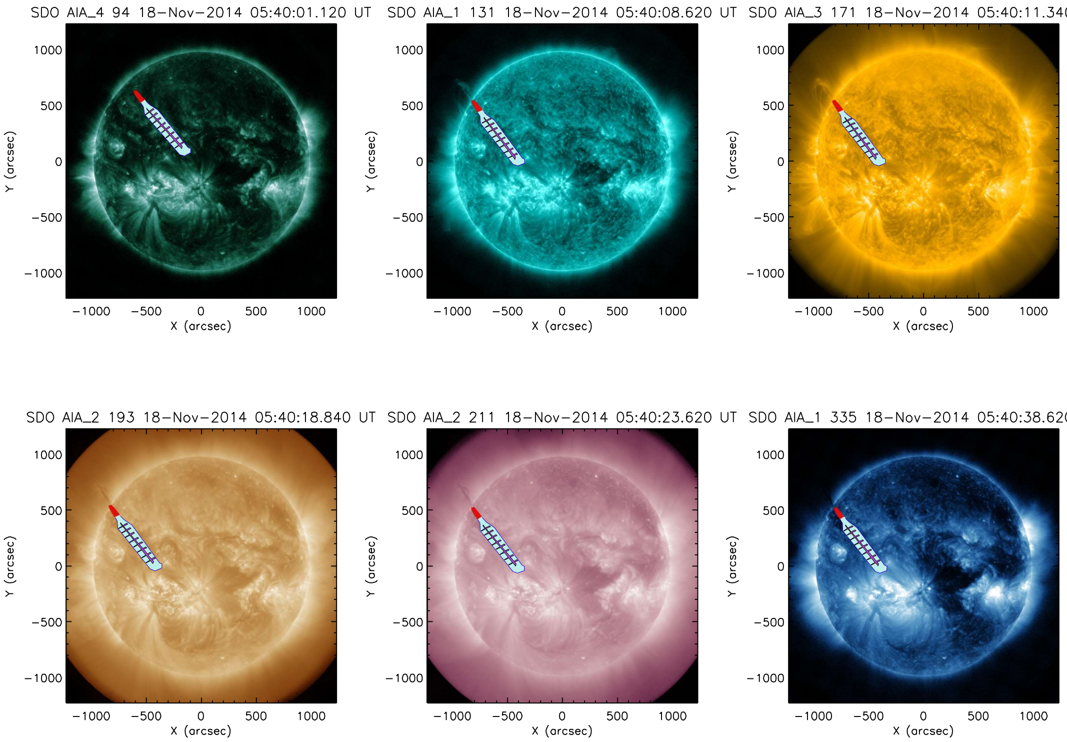

Figure 2.9: Images of six EUV filters of SDO/AIA. These six optically thin EUV filters used to understand the thermal structure of the solar atmosphere.

temperature is ranging as 5.5≤log T≤7.5 and the total emission is deduced as,

$$EM(T) = \int_{T_{min}}^{T_{max}} DEM(T)dT \tag{2.3}$$

We have defined the temperature range of the integration is 5.0≤log T≤7.3 in which the DEM solution is well-observed. For AIA data, the χ^2=1 gives the mathematically correct solution but may include non-physical negative values of the emission. To solve this the value of χ^2 increases until the positive DEM is achieved. However, it increases the computation time and increments in the noise in the higher temperature region (log T>7.0). Therefore, to overcome this problem, we adopt a more advanced version of DEM develop by (Cheung et al., 2015) using the sparse inversion method.

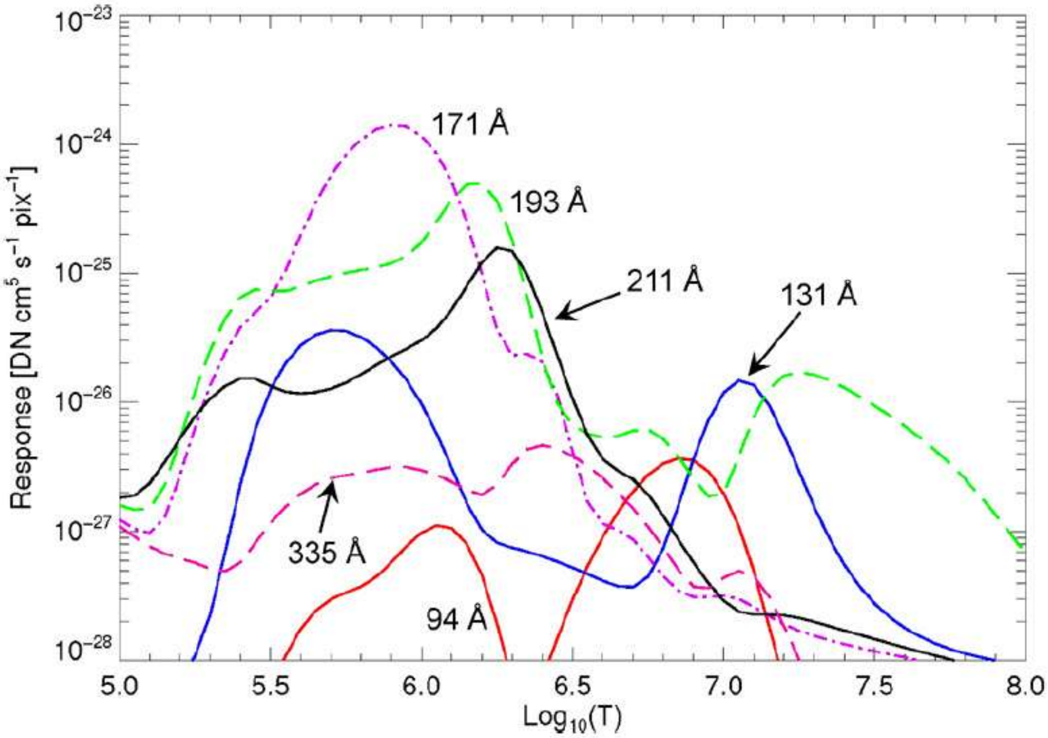

Figure 2.10: Temperature response functions for the six EUV channels of the SDO/AIA that are optically thin and dominated by iron emission lines. (Courtesy: (Lemen et al., 2012)).

2.7.2 Sparse Inversion Method

The χ^2 minimization is an ideal approach for the overdetermined system. However, the underdetermined system, the overfitting occurs with χ^2 minimum. The sparse inversion method took some data points with an underdetermined linear system (Cheung et al., 2015). The sparse inversion code is written in IDL and available in the Solarsoft is an inversion method to extract the differential emission measure (DEM) from a few data points. This method adopts the concept of sparsity and uses a simplex function to derive the solution from the optically thin SDO/AIA filters by minimizing the total emission measure (EM). The sparse inversion technique provides only the positive solution in the range of max(0,I-tol) to min(0,I+tol), where I is reconstructed intensity and tol is tolerance in the reconstructed intensities. The temperature range for sparse inversion has chosen as 5.5≤log T≤7.7 with at an interval of Δlog T=0.1. We map the DEM with six optically thin EUV filters, i.e., 94 Å, 131 Å, 171 Å, 193 Å, 211 Å, and 335 Å. The mean temperature from the DEM is calculated as,

$$T_{mean} = \frac{\int_{T_{min}}^{T_{max}} DEM(T)TdT}{\int_{T_{min}}^{T_{max}} DEM(T)dT} \tag{2.4}$$

To estimate the number density (n) from the emission measure is estimated as,

$$n = \sqrt{\frac{EM}{h}} \tag{2.5}$$

where ”h” is the depth of the region from which the emission occurred. The depth of the region along the line of sight (LOS) is assumed to be equal to the width of that region.

2.7.3 Density Estimation in the Intermediate Corona

The total brightness of solar corona is a combination of three main sources i.e., ’K’, ’F’, and ’E’ corona. These ’K’, ’F’, and ’E’ corona formed due to the Thompson scattering by the free coronal electrons, scattering due to dust, and spectral emission lines produced by heavier ions available in the coronal plasma respectively. The electron density in the solar outer corona can be determined from the measurement of linear polarization brightness produced by photospheric radiation subjected to the Thompson scattering by free coronal electrons (Brueckner et al., 1995). The STEREO/COR-1 data is used to measure the polarized brightness, which is arisen due to the Thompson scattering of photospheric photons due to free coronal electrons. This polarized brightness can be used to estimate the coronal density profile. Dolei et al. (2014) has developed a method to conjecture the coronal density profile by knowing the exact location of a feature and by measuring the polarized brightness at the same location. They suggest that in COR1 images, the measure total brightness (tB) at a pixel location where we are trying to estimate the density is a combination of three parts, i.e., the Hα emission radiated by neutral atoms from the prominence associated plasma (tB$_{H\alpha}$), the Thompson scattering by the free electron in the cool plasma (tB$_{Th}$), and Thompson scattering by coronal electron lying along the same line of sight (tB$_{Thc}$). Therefore, the total brightness measure in STEREO/COR-1 images is,

$$tB = tB_{H\alpha} + tB_{Th} + tB_{Thc} \tag{2.6}$$

To estimate the real Thompson scattering total brightness and exact density in the moving feature, we have to remove Hα and coronal brightness contribution from the COR1 intensity images. After some mathematical treatment, (Dolei et al., 2014) remove the Hα contribution. They found that the electron density is estimated by solving a quadratic equation,

$$1.57 \times 10^{-9} W^{-1} f(v) n_e^2 + n_e - \frac{tB - tB_{cor}}{< B >_d d} = 0, \tag{2.7}$$

where, $W = \frac{1}{2}\left[1 - \sqrt{1 - \frac{1}{(1+h)^2}}\right]$ in which 'h' is the height of finger in Solar radii. tB$_{cor}$=≈tB$_{Thc}$, is brightness contribution of Thompson scattering due to coronal electron. Dolei et al. (2014) have found that tB is $100-1000$ times higher than the tB$_{cor}$. Therefore, we can tB$_{cor}$ as compared to the tB. f(v) is a correction factor (f>1) that arise due to the Doppler brightness effect in Hα emission and depends upon the radial velocity of the moving feature. Rompolt (1980) computed the correction factor f(v) as a function of height above the solar surface. They found that if the speed is exceeding 100 km s^{-1} above the 1 solar radii, the correction factor is ≈4. <B>$_d$ is average brightness per electron due to Thompson scattering at a given distance from the Sun. The value of <B>$_d$ has found by using the routine 'eltheory.pro', which is available in the Solarsoft. The angle from the plane of the sky of moving feature is needed as an input in 'eltheory.pro' and it is calculated by using the tie-pointing method. d is the depth of the moving features along the line of sight, which can be approximated as the width of the feature in the plane of sky perpendicular to the radial line. After putting the above parameters (i.e., tB, tB_{cor}, $<\text{B}>_d$, d), we can estimate the number density of electron in the intermediate corona (upto 4 $R_\odot$).

2.8 Conclusions

In this chapter, we have discussed the concept of various observational methods, related instruments, and data analysis techniques that are utilized to derive various scientific results in the present thesis. Using these techniques, detailed image analysis of the solar data (EUV and coronagraphic) has been performed to explore a variety of physical parameters (e.g., density, magnetic field, etc), physics of gravity-driven instabilities, and reconnection associated plasma dynamics in solar eruptive prominences. Using a combination of the data from SDO, STEREO, BBSO Hα, WIND, etc., we analyze different types of eruptive prominences and study their dynamical plasma processes, associated eruptive phenomena, and space weather effects. The detailed scientific findings are discussed in Chapters 3-7. In the next Chapter 3, we describe the origin and evolution of MRT unstable plumes and hybrid KH-RT instability in an eruptive solar prominence.